University of Texas at El Paso
ScholarWorks@UTEP

Open Access Theses & Dissertations

2020-01-01

Positivity-Preserving Segregate-Flux Method For Infiltration Dynamics In Tumor Growth Models

Gilbert Danso Acheampong
University of Texas at El Paso

Follow this and additional works at: https://scholarworks.utep.edu/open_etd

Part of the Mathematics Commons

Recommended Citation

Acheampong, Gilbert Danso, "Positivity-Preserving Segregate-Flux Method For Infiltration Dynamics In Tumor Growth Models" (2020). *Open Access Theses & Dissertations*. 3075.
https://scholarworks.utep.edu/open_etd/3075

This is brought to you for free and open access by ScholarWorks@UTEP. It has been accepted for inclusion in Open Access Theses & Dissertations by an authorized administrator of ScholarWorks@UTEP. For more information, please contact lweber@utep.edu.

POSITIVITY-PRESERVING SEGREGATE-FLUX METHOD FOR INFILTRATION DYNAMICS IN TUMOR GROWTH MODELS

GILBERT DANSO ACHEAMPONG

Master's Program in Mathematics

APPROVED:

Xianyi Zeng, Ph.D., Chair.

Granville Sewell, Ph.D.

Natasha Sharma, Ph.D.

Crites Stephen, Ph.D.
Dean of the Graduate School

©Copyright

by

Gilbert Danso Acheampong

2020

to my

FAMILY

with love

POSITIVITY-PRESERVING SEGREGATE-FLUX METHOD FOR INFILTRATION DYNAMICS IN TUMOR GROWTH MODELS

by

GILBERT DANSO ACHEAMPONG

THESIS

Presented to the Faculty of the Graduate School of

The University of Texas at El Paso

in Partial Fulfillment

of the Requirements

for the Degree of

MASTER OF SCIENCE

Department of Mathematical Sciences

THE UNIVERSITY OF TEXAS AT EL PASO

August 2020

Acknowledgements

Glory be to Jehovah Elohim for His goodness throughout my education.

I would like to express my sincerest gratitude to my Advisor, Dr. Xianyi Zeng for introducing me to this amazing area of research. His patience and genuine concern throughout the thesis was really remarkable.

Also, I would like to thank my thesis committee, Dr. Granville Sewell and Dr. Natasha Sharma for their invaluable time, even in the heap of the Covid-19 pandemic. I am very grateful.

I want to thank The University of Texas at El Paso and the Mathematical Sciences Department professors and staff, especially Dr. Mariani (Chair), Dr. Helmut Knaust, Maria Barraza-Rios, Maria Salandiya and Valerie Dominguez for their hard work and dedication, which in one way or the other provided me the means to complete this degree successfully.

And finally, to my colleagues, family and fiends whose contributions in various ways brought this journey into fruition. I say thank you to all.

NOTE: This thesis was submitted to my Supervising Committee on the July 20, 2020.

Abstract

We study the positivity preserving property and an incompressibility condition in a recently proposed tumor growth model as well as its numerical simulations. In this model, the biological process is described by a free-boundary problem of hyperbolic equations that govern the in-tumor motion of cancer cells and the infiltration of immune cells. Particularly, due to an assumption that cells take constant volume (the incompressibility condition), the tumor growth/shrinkage is closely correlated to the magnitude of infiltration of immune cells into the tumor.

Despite the fact that previous simulation results largely reproduced experimental data, there remain unanswered questions that are crucial for the justification of such models. In this thesis, we make a first step to address two such questions, namely preserving the positivity of variables that represent cell number densities and the incompressibility condition, from both a mathematical perspective and a numerical point of view. In particular, we first show that under certain assumptions, the analytic solutions to the mathematical model must preserve positive cell number densities as well as maintaining the cell incompressibility. Then we examine a recently proposed segregate-flux finite volume method, which is designed preserves numerical cell incompressibility, and show that it also positivity-preserving under minor modifications.

Table of Contents

Page

Acknowledgements v

Abstract vi

Table of Contents vii

Chapter

Introduction 1

1 A Tumor Growth Problem 4

1.1 Model in normalized coordinates 5

1.2 Initial and boundary conditions 6

1.3 A schematic description of the model and open problems 7

1.4 Nomenclature 8

2 The Numerical Method 9

2.1 FVM for the model problem, DTCL, and DGCL 10

2.2 Finite volume discretization using segregated fluxes 12

2.3 Numerical Examples 13

3 Preliminary Mathematical Analysis 16

3.1 Characteristic analysis of the G-equation 16

3.2 Characteristic analysis of the M-equation 18

3.3 The incompressibility assumption 19

4 Numerical Positivity Preserving 21

4.1 Advection equation with first-order upwind FVM 21

4.2 The first-order fluxes for the model problem 22

4.3 The PPM flux for the model problem 24

4.4 An enhanced PPM flux with synchronized limiter 26

5 Conclusions 29

References 30
Curriculum Vitae 33

Introduction

Tumors are complex tissues that contain cancer cells and other variety of cells including those in the immune system [13, 15]. For the past decades, researchers from different fields have relied on mathematical modeling to complement their experimental studies; by way of analyzing the complex biology of tumors in order to extract simple principles useful for designing novel diagnostic and treatment strategies [14].

Numerous investigations show that immune cell infiltration plays a crucial role in tumor growth in many types of cancers [6, 8]. However, existing lab and clinical studies have led to seemingly conflicting observations. On the one hand, local contact between immune cells and tumor (cancer) cells leads to the demise of the latter; on the other hand, when too many immune cells enter (infiltrate) the tumor in a short period of time they tend to enlarge the region the tumor occupies and results in aggressive tumor growth [7, 9, 11]. To this end, mathematical modeling has become an indispensable tool to gain a deeper understanding of this phenomenon and several models based on partial differential equations (PDE) have been developed in the past decades.

Recently, B. Niu et al. [1] proposed a free-boundary PDE model for immune cell infiltration that is driven by PDGF (platelet-derived growth factor) into glioma tumor. This model is motivated by the conservation law of incompressible fluids, and it enjoys the advantage over others in its explicitly capturing the (moving) tumor boundary hence one easily relates the migration of various types of cells to the growth or shrinkage of the tumor domain. However, it also complicates both the mathematical analysis and the numerical investigation using classical methodologies.

Three different cell species are considered in this model: the glioma cells (G), the necrotic cells (H), and the immune cells (M); among the three, G and H are native ones and their domain define the tumor region, whereas M is the infiltration species whose motion is guided by the gradient of chemoattractant (A) that is secreted by glioma cells. This procedure is described by

the equations below in the spherical symmetry case:

$$\frac{\partial G(r,t)}{\partial t}+\frac{1}{r^2}\frac{\partial}{\partial r}\left[r^2G(r,t)V(r,t)\right]=\lambda G(r,t)-\mu G(r,t)\ ,$$
$$\frac{\partial H(r,t)}{\partial t}+\frac{1}{r^2}\frac{\partial}{\partial r}\left[r^2H(r,t)V(r,t)\right]=\mu G(r,t)-\delta H(r,t)\ ,$$
$$\frac{\partial M(r,t)}{\partial t}+\frac{1}{r^2}\frac{\partial}{\partial r}\left[r^2M(r,t)V(r,t)\right]=-\frac{\alpha}{r^2}\frac{\partial}{\partial r}\left[r^2M(r,t)\frac{\partial A(r,t)}{\partial r}\right]-\rho M(r,t)\ ,$$

on a moving domain $0\le r\le R(t)$ for the cell number densities and:

$$\frac{\partial A(r,t)}{\partial t}=\frac{\nu}{r^2}\frac{\partial}{\partial r}\left[r^2\frac{\partial A(r,t)}{\partial r}\right]+\frac{mG(r,t)}{\beta+G(r,t)}-\gamma A(r,t)$$

on the unbound domain $0\le r<\infty$ for the chemoattractant concentration. Here the radius of the tumor is denoted $R(t)$ and the in-tumor migration velocity for native cells (G and H) is $V(r,t)$. In particular, one has $R'(t)=V(R(t),t)$ and an integral equation for V is obtained by summing all three cell-species equations and replacing $G+H+M$ by a constant θ that represents the total number of cells per unit volume:

$$\frac{1}{r^2}\frac{\partial}{\partial r}\left[r^2V(r,t)\theta+\alpha r^2\frac{\partial A(r,t)}{\partial r}M(r,t)\right]=\lambda G(r,t)-\delta H(r,t)-\rho M(r,t)\ .$$

The Greek letters are model parameters describing proliferation, apoptosis, and necrosis of cells whose values are typically obtained by independent studies.

An important assumption in deriving the V-equation is the incompressibility of the cells:

$$G+H+M=\theta\ ,$$

whereas whether it will be satisfied by the solutions to the model remains an open question. Nevertheless, motivated by preserving the cell incompressibility at the discrete level, a segregate-flux finite volume method (FVM) is proposed recently [2] and the authors show that this method outperform conventional FVMs and deliver convergence numerical solutions.

An interesting observation from the previous computational study is that even in extreme scenarios, such as when a strong discontinuity presents and when some cell number densities diminishes towards zero, all numerical solutions remain positive. Such a phenomenon is known as

positivity-preserving in the literature; whereas unlike many other contexts in which the positivity-preserving property is usually discussed, no maximum principle can be derived in the present settings. In fact, whether the solutions to the mathematical problem will stay positive remains an open question, too, despite the fact that it makes perfect biological sense – all cell number densities should be positive. To gain a better understanding of the model, the main purpose of this thesis is to make an attempt in providing mathematical justification of the two important properties: positivity-preserving and cell incompressibility of both the mathematical model and the segregate-flux method.

To this end, the rest of the thesis is organized as follows. A slightly simplified model problem that contains two instead of three cell species is introduced in Chapter 1. In this chapter, we also describe the technique to convert the free-boundary problem to a fixed-boundary one using a normalized coordinate system. The numerical scheme is reviewed in Chapter 2, which includes a general FVM strategy as well as the segregate-flux scheme. Mathematical analysis of the positivity-preserving and cell incompressibility properties are proved in Chapter 3 with the assumption that solutions exist in the strong sense. Next, the positivity-preserving property of the segregate-flux FVM is discussed in Chapter 4, where a simple fix is proposed to ensure that the method computes positive cell number densities at the new time step providing that the they are positive at the previous time step. Finally, we conclude the thesis and speculate on the future directions in Chapter 5.

Chapter 1

A Tumor Growth Problem

For simplicity, we consider a two-species system with an additional variable for the velocity:

$$\frac{\partial G}{\partial t} + \frac{1}{r^2}\frac{\partial}{\partial r}\left[r^2 G V\right] = f\,, \tag{1.1a}$$

$$\frac{\partial M}{\partial t} + \frac{1}{r^2}\frac{\partial}{\partial r}\left[r^2 M(V+u)\right] = h\,, \tag{1.1b}$$

$$\frac{1}{r^2}\frac{\partial}{\partial r}\left[r^2 V + r^2 u M\right] = f + h\,. \tag{1.1c}$$

Here r is the radial coordinate inside the tumor: $0 \le r \le R(t)$ with $R(t)$ being the tumor radius at time t. The upper case letters denote dependent variables: G is the number density of the native cells (cancer cell, necrotic cell, etc.) in the tumor, M is the number density of the infiltrating cells (such as the immune cells), V is the velocity of the native cells, and R is the tumor radius. For this problem, G and M are considered dimensionless, i.e., they are normalized by the constant total cell number per unit volume $\theta > 0$; hence for a biologically relevant solution it is natural to required that $0 \le G, M \le 1$. The lower case letters denote either the independent variables such as r and t, or prescribed quantities or functions. In particular, u is the infiltration velocity that determines how M enters or exits the domain. The source terms f and h are known functions of G and M that model the proliferation, apoptosis, and interaction among cell species. For simplicity, we suppose there exists a positive constant L such that:

$$\begin{aligned} f = \hat{f}(G,M)G\,,\ h = \hat{h}_1(G,M)G + \hat{h}_2(G,M)M\,, \\ \text{where}\quad \left|\hat{f}\right|, \left|\hat{h}_1\right|, \left|\hat{h}_2\right| \le L \quad \text{and} \quad \hat{h}_1 \ge 0 \quad \forall (G,M) \in [0,\,1]^2\,. \end{aligned} \tag{1.2}$$

The biological motivation behind these assumptions can be found in [21]. In short, the hat functions represents the growth/decay rate or conversion rate within and between cell species, which are typically bounded functions as observed in lab studies.

The tumor grows at a rate determined by the velocity V at the outer boundary:

$$R'(t) = V(R(t),t)\,. \tag{1.3}$$

And in deriving the velocity equation (1.1c), the cell incompressibility is assumed:

$$G+M \equiv 1\,. \tag{1.4}$$

As in many mathematical models of similar biological systems [22–24], the incompressibility identity (1.4) is *assumed* rather than *enforced* to derive the velocity equation. Whether the solutions satisfy the incompressibility assumption remains an open probem, but in Chapter 3, we will prove it in the case of classical solutions.

To see why (1.4) should hold, we introduce the total cell number variable $\Theta \stackrel{\text{def}}{=\!=} G+M$. Adding (1.1a) and (1.1b) and incorporating (1.1c), one arrives at an equation for Θ:

$$\frac{\partial \Theta}{\partial t} + \frac{1}{r^2}\frac{\partial}{\partial r}\left[r^2(\Theta-1)V\right] = 0\,. \tag{1.5}$$

Clearly, $\Theta \equiv 1$ (the incompressibility constraint) solves (1.5). This equation is called the totality conservation law (TCL); and if a numerical discretization for (1.1) gives rise to a consistent discretization of (1.5), i.e., a formula that only depends on Θ but not on how it splits into G and M, the method is said to satisfy the TCL discretely, or DTCL. Applying the conventional upwind method to solve (1.1), for example, does not satisfy DTCL because G and M are carried by velocities that may have opposite directions, see a brief discussion in Chapter 2 and a more thorough exposition in [2].

1.1 Model in normalized coordinates

To avoid dealing with a changing domain, we normalize the radial coordinate by the change of variables $(r,\,t) \mapsto (\eta,\,\tau) = (r/R(t),\,t)$. To this end, the governing equations are converted to the

conservation form:

$$\frac{\partial(\eta^2R^2G)}{\partial\tau}+\frac{\partial}{\partial\eta}\left[\left(\frac{V}{R}-\frac{\eta R'}{R}\right)\eta^2R^2G\right]=\eta^2R^2f-\eta^2R'RG\,, \tag{1.6a}$$

$$\frac{\partial(\eta^2R^2M)}{\partial\tau}+\frac{\partial}{\partial\eta}\left[\left(\frac{V}{R}-\frac{\eta R'}{R}+\frac{u}{R}\right)\eta^2R^2M\right]=\eta^2R^2h-\eta^2R'RM\,, \tag{1.6b}$$

$$\frac{1}{\eta^2}\frac{\partial}{\partial\eta}\left[\eta^2\left(\frac{V}{R}+\frac{u}{R}M\right)\right]=f+h\,. \tag{1.6c}$$

for all $\eta\in[0,\,1]$, $\tau\in[0,\,T]$ with some $T>0$. The radius $R(\tau)$ is determined by:

$$R'(\tau)=V(1,\,\tau)\,. \tag{1.6d}$$

Similarly, the TCL in the normalized coordinates is:

$$\frac{\partial(\eta^2R^2\Theta)}{\partial\tau}+\frac{\partial}{\partial\eta}\left[\eta^2R(\Theta-1)V\right]-\frac{\partial}{\partial\eta}\left[\eta^3R'R\Theta\right]=-\eta^2R'R\Theta\,. \tag{1.7}$$

Setting $\Theta=1$, this equation reduces to:

$$\frac{\partial(\eta^2R^2)}{\partial\tau}-\frac{\partial}{\partial\eta}\left[\eta^3R'R\right]=-\eta^2R'R\,, \tag{1.8}$$

which holds trivially at the continuous level and is called the geometric conservation law (GCL). At discrete level, however, a discrete version of the GCL may not be satisfied by the numerical method. If the method satisfies a discrete version of (1.8), it is said to satisfy the discrete geometric conservation law (DGCL).

1.2 Initial and boundary conditions

The tumor growth problem (1.6) is completed by proper initial and boundary conditions. At $\tau=0$, the initial data for cell number densities satisfy:

$$G(\eta,0)\geq0\,,\quad M(\eta,0)\geq0\,,\quad G(\eta,0)+M(\eta,0)=1\,,\quad\forall\,0\leq\eta\leq1\,. \tag{1.9}$$

No initial data is needed for V, because (1.6c) does not contain an inertia term; and V can be fully determined by integrating (1.6c):

$$V(\eta,\tau)=\frac{R}{\eta^2}\int_0^\eta s^2(f(s,\tau)+h(s,\tau))ds-u(\eta,\tau)M(\eta,\tau)\,. \tag{1.10}$$

Here we write $f(s,\tau) = f(G(s,\tau), M(s,\tau))$ and $h(s,\tau) = h(G(s,\tau), M(s,\tau))$ for short. In addition, the zero boundary condition for velocity at the tumor center is assumed and it comes from the spherical symmetry assumption:

$$V(0,\tau) = 0\,, \quad \forall\, 0 \le \tau \le T\,. \tag{1.11a}$$

The boundary conditions for cell numbers at $\eta = 0$ is the no-flux condition, which is again due to the spherical symmetry assumption:

$$\frac{\partial G(0,\tau)}{\partial \eta} = \frac{\partial M(0,\tau)}{\partial \eta} = 0\,, \quad \forall\, 0 \le \tau \le T\,. \tag{1.11b}$$

At the right boundary, the local velocity for G is $\frac{V(1,\tau)}{R(\tau)} - \frac{R'(\tau)}{R(\tau)} = 0$ thus no boundary condition is required; and the classical characteristic condition is specified for M:

$$M(1,\tau) = m_{\text{bc}}(\tau) \quad \text{if} \quad u(1,\tau) < 0\,, \quad \forall\, 0 \le \tau \le T\,, \tag{1.11c}$$

where m_{bc} is the prescribed ambient immune cell number density.

1.3 A schematic description of the model and open problems

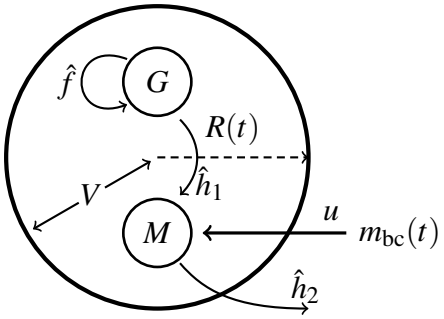

The model can be described schematically in the diagram on the right. When too many immune cells enter the domain (the arrow with u), especially if the infiltration outweighs the decay of cells inside the tumor, the total tumor number increases and thusly the tumor expands due to the incompressibility of cells; and vice versa. In the diagram, the directions of the arrows are motivated by the typical observation that G tends to reproduce itself very quickly ($\hat{f} > 0$), whereas the immune cells tend not to reproduce ($\hat{h}_2 < 0$). The positivity of cell number densities and incompressibility are two important features of this model. Between the two, this thesis focuses on the positivity from both a mathematical perspective (Chapter 3) and a numerical point of view (Chapter 4). Note that the incompressibility is addressed by numerical

methods in the literature [2], see also the next chapter for a review, a mathematical justification is nevertheless provided in Chapter 3.

1.4 Nomenclature

At the end of this section, we summarize the nomenclature that will be used throughout the thesis, among which some have already been used before whereas others will show up shortly.

Symbol	Explanation	Symbol	Explanation
η	spatial abscissa	Θ	total cell number defined as G+M
τ	temporal ordinate	V	velocity variable
$\Delta\eta$	uniform interval size	u	prescribed infiltration velocity
$\Delta\tau^n$	time step between τ^n and τ^{n+1}	$\mathscr{F}^{\mathrm{upw}}$	the upwind flux function
G	cell number variable for the cancer cells	ξ	characteristic function
M	cell number variable for the immune cells	$\mathscr{E}$	energy functional

Chapter 2

The Numerical Method

Due to the hyperbolic nature of (1.1) and (1.6), the finite volume methods (FVM) [25] are adopted for numerical simulations. To illustrate the basic idea of general finite volume discretizations, let us consider a uniform gird of $\eta \in [0,\ 1]$ with N_η intervals[1]. The interval size, the interval faces, and the interval centers are denoted $\Delta\eta = 1/N_\eta$, $\eta_j = j\Delta\eta$, and $\eta_{j-\frac{1}{2}} = \left(j-\frac{1}{2}\right)\Delta\eta$, respectively.

Consider a scalar conservation law for a generic conserved quantity X:

$$\frac{\partial X}{\partial \tau} + \frac{\partial F(X)}{\partial \eta} = 0\,, \quad X = X(\eta,\tau)\,,\ 0 \le \eta \le 1\,,\ 0 \le \tau \le T\,. \tag{2.1}$$

The spatial discretization can be derived by integrating (2.1) over each interval to obtain:

$$\frac{dX_{j-\frac{1}{2}}}{d\tau} + \frac{1}{\Delta\eta}\left(F_j - F_{j-1}\right) = 0\,, \tag{2.2}$$

where $X_{j-\frac{1}{2}}$ approximates the interval-averaged solution:

$$X_{j-\frac{1}{2}}(\tau) \approx \frac{1}{\Delta\eta}\int_{\eta_{j-1}}^{\eta_j} X(\eta,\tau)d\eta\,, \tag{2.3}$$

and $F_j()$ denotes a numerical flux that approximates $F(X(\eta_j,\tau))$. Because no direct approximation to $X(\eta_j,\tau)$ is provided in FVMs, F_j is usually computed from nearby interval-averaged solutions. For example, if $F()$ describes the transport by a constant velocity u, i.e., $F(X) = uX$, the well-known first-order upwind flux by Godunov [26] is defined as:

$$F_j = \mathscr{F}^{\text{upw}}(X_{j-\frac{1}{2}}, X_{j+\frac{1}{2}}; u) \overset{\text{def}}{=\!=} \begin{cases} uX_{j-\frac{1}{2}} & \text{if } u \ge 0\,, \\ uX_{j+\frac{1}{2}} & \text{if } u < 0\,. \end{cases} \tag{2.4}$$

[1] In classical literature for finite volume methods, these intervals are referred to as "cells"; here, however, we reserve the word "cell" for dependent variables and thusly use "interval" for the mesh entities instead.

Other numerical flux functions that are relevant to this study include the MUSCL scheme by van Leer [10] and the PPM scheme by Colella and coworkers [20, 27]. In particular, a segregate flux method is proposed by Zeng et al. to treat infiltration dynamics [2], which will be the underlying numerical scheme in this work and it is briefly reviewed next.

2.1 FVM for the model problem, DTCL, and DGCL

To get an idea why direct application of classical methods are not suitable for solving (1.6), we will demonstrate in this section that using upwind flux for both G and M-equations, and using forward-Euler to march the solutions in time will not satisfy the discrete totality conservation law and the discrete geometric conservation law.

First of all, the semi-discretized approximations of (1.6) need to take into account of the weighting by r^2, hence they're defined as:

$$G_{j-\frac{1}{2}}(\tau) \approx \frac{1}{\Delta\eta\,\eta_{j-\frac{1}{2}}^2 R^2} \int_{\eta_{j-1}}^{\eta_j} \eta^2 R^2 G(\eta,\tau) d\eta \ , \tag{2.5a}$$

$$M_{j-\frac{1}{2}}(\tau) \approx \frac{1}{\Delta\eta\,\eta_{j-\frac{1}{2}}^2 R^2} \int_{\eta_{j-1}}^{\eta_j} \eta^2 R^2 M(\eta,\tau) d\eta \ , \tag{2.5b}$$

where the half-integer subscripts indicate they are interval-centered variables. In contrast, integer subscripts are used for nodal quantities such as the velocities:

$$V_j(\tau) \approx V(\eta_j,\tau) \ , \quad u_j(\tau) \approx u(\eta_j,\tau) \ . \tag{2.6}$$

To this end, the semi-discretization of the system (1.6) for $G_{j-\frac{1}{2}}$, $M_{j-\frac{1}{2}}$, and V_j is given by:

$$\frac{d(\eta_{j-\frac{1}{2}}^2 R^2 G_{j-\frac{1}{2}})}{d\tau} + \frac{1}{\Delta\eta}\left[F_j^G - F_{j-1}^G\right] = \eta_{j-\frac{1}{2}}^2 R^2 f_{j-\frac{1}{2}} - \eta_{j-\frac{1}{2}}^2 R' R G_{j-\frac{1}{2}} \ , \tag{2.7a}$$

$$\frac{d(\eta_{j-\frac{1}{2}}^2 R^2 M_{j-\frac{1}{2}})}{d\tau} + \frac{1}{\Delta\eta}\left[F_j^M - F_{j-1}^M\right] = \eta_{j-\frac{1}{2}}^2 R^2 h_{j-\frac{1}{2}} - \eta_{j-\frac{1}{2}}^2 R' R M_{j-\frac{1}{2}} \ , \tag{2.7b}$$

$$V_0 = 0 \ , \quad \eta_j^2 R V_j + F_{u,j}^M = \sum_{k=1}^{j} \Delta\eta \left(\eta_{k-\frac{1}{2}}^2 R^2 f_{k-\frac{1}{2}} + \eta_{k-\frac{1}{2}}^2 R^2 h_{k-\frac{1}{2}}\right) \ . \tag{2.7c}$$

Here the fluxes F_j^G and F_j^M approximates $(\frac{V}{R}-\frac{\eta R'}{R})\eta^2R^2G$ and $(\frac{V}{R}-\frac{\eta R'}{R}+\frac{u}{R})\eta^2R^2M$ at η_j, respectively; and they're left unspecified for the moment. Similarly, the flux $F_{u,j}^M$ in the velocity equation approximates $u\eta^2RM$ at η_j.

Using the upwind flux directly to compute F_j^G and F_j^M, one needs to apply $\mathscr{F}^{\text{upw}}$ to the conserved quantities (η^2R^2G and η^2R^2M) with the velocities $\frac{V}{R}-\frac{\eta R'}{R}$ and $\frac{V}{R}-\frac{\eta R'}{R}+\frac{u}{R}$, respectively:

$$
\begin{aligned}
F_j^G &= \mathscr{F}^{\text{upw}}\left(\eta_{j-\frac{1}{2}}^2R^2G_{j-\frac{1}{2}},\eta_{j+\frac{1}{2}}^2R^2G_{j+\frac{1}{2}};\frac{V_j}{R}-\frac{\eta_jR'}{R}\right)\,,\\
F_j^M &= \mathscr{F}^{\text{upw}}\left(\eta_{j-\frac{1}{2}}^2R^2M_{j-\frac{1}{2}},\eta_{j+\frac{1}{2}}^2R^2M_{j+\frac{1}{2}};\frac{V_j}{R}-\frac{\eta_jR'}{R}+\frac{u_j}{R}\right)\,.
\end{aligned}
$$

To satisfy DTCL, adding F_j^G and F_j^M needs to form a consistent flux for $\Theta=G+M$, except for M carried by the infiltration velocity u, which is eventually balanced out by a careful chosen $F_{u,j}^M$ in the velocity equation. This, however, cannot be achieved by the two upwind fluxes above, as the two local velocities may have different signs; for example, supposing $\frac{V_j}{R}-\frac{\eta_jR'}{R}>0$ and $\frac{V_j}{R}-\frac{\eta_jR'}{R}+\frac{u_j}{R}<0$, one obtains:

$$
F_j^G+F_j^M=\left(\frac{V_j}{R}-\frac{\eta_jR'}{R}\right)\left(\underline{\eta_{j-\frac{1}{2}}^2R^2G_{j-\frac{1}{2}}+\eta_{j+\frac{1}{2}}^2R^2M_{j+\frac{1}{2}}}\right)+\frac{u_j}{R}\eta_{j+\frac{1}{2}}^2R^2M_{j+\frac{1}{2}}\,,
$$

Note that the underlined part does not sum into an expression of either $\Theta_{j-\frac{1}{2}}$ or $\Theta_{j+\frac{1}{2}}$, which is technically required by DTCL.

The semi-discretization (2.7) needs to be complemented by a time-integrator, for which purpose the explicit forward Euler (FE) method is chosen throughout the thesis. Hence the fully discretized method updating the solutions from τ^n to $\tau^{n+1}=\tau^n+\Delta\tau^n$ now reads:

$$
\frac{\eta_{j-\frac{1}{2}}^2\left[(R^{n+1})^2G_{j-\frac{1}{2}}^{n+1}-(R^n)^2G_{j-\frac{1}{2}}^n\right]}{\Delta\tau^n}+\frac{F_j^{G,n}-F_{j-1}^{G,n}}{\Delta\eta}=\eta_{j-\frac{1}{2}}^2(R^n)^2f_{j-\frac{1}{2}}^n-\eta_{j-\frac{1}{2}}^2R'^nR^nG_{j-\frac{1}{2}}^n,\quad\text{(2.8a)}
$$

$$
\frac{\eta_{j-\frac{1}{2}}^2\left[(R^{n+1})^2M_{j-\frac{1}{2}}^{n+1}-(R^n)^2M_{j-\frac{1}{2}}^n\right]}{\Delta\tau^n}+\frac{F_j^{M,n}-F_{j-1}^{M,n}}{\Delta\eta}=\eta_{j-\frac{1}{2}}^2(R^n)^2h_{j-\frac{1}{2}}^n-\eta_{j-\frac{1}{2}}^2R'^nR^nM_{j-\frac{1}{2}}^n,\quad\text{(2.8b)}
$$

$$
V_0^n=0\,,\quad \eta_j^2RV_j^n+F_{u,j}^{M,n}=\sum_{k=1}^{j}\Delta\eta\left(\eta_{k-\frac{1}{2}}^2(R^n)^2f_{k-\frac{1}{2}^n}+\eta_{k-\frac{1}{2}}^2(R^n)^2h_{k-\frac{1}{2}}^n\right)\,.\quad\text{(2.8c)}
$$

Direct application of FE, however, will not ensure DGCL. To see why, suppose R'^n is already computed and one update R by:

$$R^{n+1} = R^n + \Delta\tau^n R'^n \,,$$

then the numerical discretization of the GCL (1.8) becomes for each $1 \leq j \leq N_\eta$:

$$\frac{\eta^2_{j-\frac{1}{2}}(2\Delta\tau^n R'^n + \Delta\tau^n (R'^n)^2)}{\Delta\tau^n} - \mathscr{D}_j[\eta^3 R'^n R^n] = -\eta^2_{j-\frac{1}{2}} R' n R^n \,, \tag{2.9}$$

where $\mathscr{D}_j$ approximates the spatial derivative at η_j and it results from the spatial discretization. Clearly, if DGCL is satisfied then the latest equality always holds; but it means that the spatial discretization $\mathscr{D}_j$ must explicitly depend on the time step size $\Delta\tau^n$, which is highly undesirable.

2.2 Finite volume discretization using segregated fluxes

These numerical difficulties are resolved by the segregated-flux method [2]. Skipping the details, the fundamental idea is to compute the flux associated with each velocity component separately:

$$F^G_j = F^G_{V,j} + F^G_{R',j} \,, \quad F^M_j = F^M_{V,j} + F^M_{R',j} + F^M_{u,j} \,, \tag{2.10}$$

Here the terms on the right hand sides approximated different flux components:

$$F^X_{V,j} \approx V\eta^2 RX\big|_{\eta=\eta_j} \,, \quad F^X_{R',j} \approx -\eta^3 R' RX\big|_{\eta=\eta_j} \,, \quad F^X_{u,j} \approx u\eta^2 RX\big|_{\eta=\eta_j} \,, \tag{2.11}$$

where X is again a generic variable representing the transported quantity such as G and M.

The fluxes associated with the spatially varying velocities V or u are then computed by applying any chosen numerical flux (we use upwind flux in this thesis for simplicity) to the primitive variable X instead of the conservative one $\eta^2 R^2 X$:

$$F^X_{W,j} = \eta^2_j R \mathscr{F}^{\text{upw}}(X_{j-\frac{1}{2}}, X_{j+\frac{1}{2}}; W_j) \,, \tag{2.12}$$

where W is a generic variable representing the nodal velocities such as V or u. By doing so, one clearly sees that $F^M_{V,j} + F^G_{V,j} = F^\Theta_{V,j}$, and that $F^M_{V,j}$ and $F^M_{u,j}$ can take M from different directions, both of which are crucial in achieving DTCL by the final numerical method.

Further enhancements are required to ensure DGCL. First of all, to eliminate the issue of a $\Delta\tau^n$-dependent spatial discretization at the end of the previous section, one computes R'^n and R^{n+1} according to:

$$R'^n = \left(1 - \frac{1}{4}\Delta\eta^2\right)^{-1} V_{N_\eta}^n, \qquad \frac{(R^{n+1})^2 - (R^n)^2}{2\Delta\tau^n R^n} = R'^n \,, \tag{2.13}$$

in the case of the FE time-integrator. If other time-integrators are used, such as the implicit backward Euler method, the radius updating formula also needs to be modified accordingly. Note that the factor $(1-\Delta\eta^2/4)^{-1}$ is generally not required for deriving a $\Delta\tau^n$-independent spatial discretization, but it helps eliminate some spurious influx at the tumor boundary.

Lastly, as the operator $\mathscr{D}_j$ of (2.9) applies to a cubic profile and it is a direct result of the fluxes $F^X_{R',j}$, one needs at least a third-order accurate method to compute the latter to ensure (2.9) holds at the discrete level. To this end, the last piece in the enhanced method is to use the piecewise-parabolic method (PPM) [20, 27] to compute $F^G_{R',j}$ and $F^M_{R',j}$. More details will be offered in Chapter 4, in which we improvise on further enhancements to ensure positivity of cell number solutions under appropriate Courant conditions to compute the time step size $\Delta\tau^n$.

2.3 Numerical Examples

In this section we demonstrate that the segregate-flux method is not only able to numerically preserve the incompressibility, but also maintain the positivity of cell number solutions. For simplicity, we suppose $\hat{f} \equiv -1$, $\hat{h}_1 \equiv 1$, and $\hat{h}_2 \equiv -1$; thus the equations (1.1) read:

$$\frac{\partial G}{\partial t} + \frac{1}{r^2}\frac{\partial}{\partial r}\left[r^2 G V\right] = -G \,, \tag{2.14a}$$

$$\frac{\partial M}{\partial t} + \frac{1}{r^2}\frac{\partial}{\partial r}\left[r^2 M(V+u)\right] = G - M \,, \tag{2.14b}$$

$$\frac{1}{r^2}\frac{\partial}{\partial r}\left[r^2 V + r^2 u M\right] = -M \,. \tag{2.14c}$$

Seeing that in traditional numerical solutions to hyperbolic conservation laws, violation of positivity usually initiates from the vicinity of discontinuities where spurious oscillations typi-

cally occur, we consider the following initial data with piecewise constant cell numbers:

$$R(0) = 1.0\,, \quad G(r,t) = \begin{cases} 0.9 & 0 < r < 0.5 \\ \\ 0.1 & 0.5 < r < 1 \end{cases}, \quad M(r,t) = \begin{cases} 0.1 & 0 < r < 0.5 \\ \\ 0.9 & 0.5 < r < 1 \end{cases}. \tag{2.15}$$

We consider an infiltration velocity that tends to shrink the tumor:

$$u(r,t) = \frac{rt^2}{4m_{\text{bc}}}\,, \tag{2.16}$$

and one that tends to expand the tumor:

$$u(r,t) = -\frac{rt^2}{4m_{\text{bc}}}\,, \tag{2.17}$$

where $m_{\text{bc}} \equiv 0.9$ is the constant ambient immune cell number density in both cases.

Computing the time step size using a fixed Courant number 0.8, the radius growth histories of the two problems on a sequence of uniform grids with number of intervals $N_\eta = 20$, $N_\eta = 40$, and $N_\eta = 80$ are plotted in Figures 2.1. Note that in Figure 2.1b the radius is not monotonically

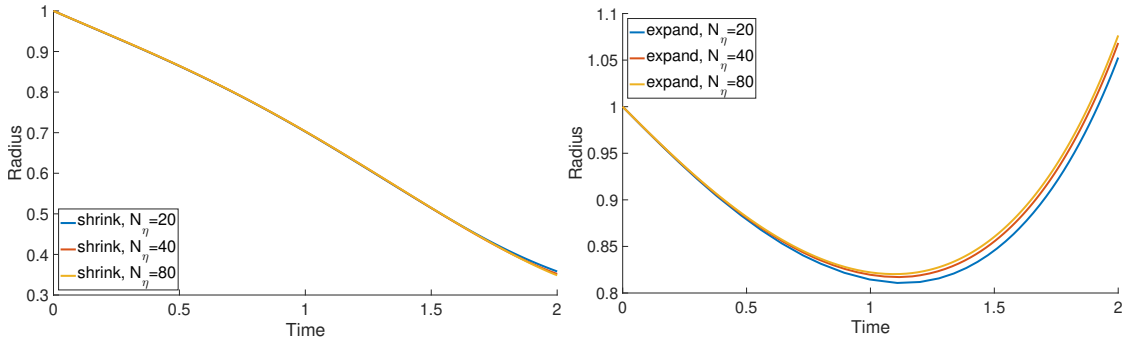

(a) The "shrinking" problem (2.16).

(b) The "expanding" problem (2.17).

Figure 2.1: The radius histories of the two tumor problems on a sequence of three uniform grids.

growing. The reason is that although the immune cells N infiltrate into the tumor, that is $u(R,t) < 0$ by (2.17), the aggregate source term (sum of the right-hand sides of the cell-number equations) removes cells from the tumor – thus the tumor initially shrinks and later expands as the infiltration velocity increases.

The cell number solutions at different times with an equal interval 0.2 computed on the finest grid ($N_\eta = 80$) are plotted in Figure 2.2, where the solutions to the "shrinking" problem are plotted in the left column and that to the "expanding" problem are plotted in the right column. From these plots, we see that: (a) the solutions are essentially oscillation free, especially nearby

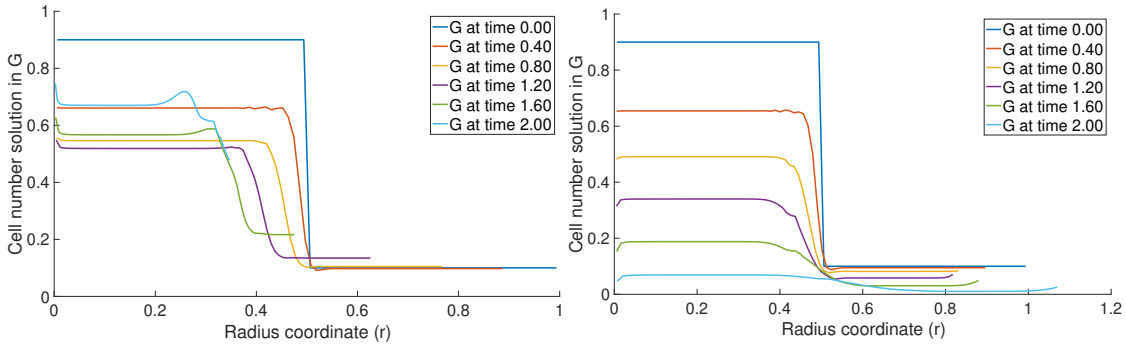

(a) Solution in G for the "shrinking" problem.

(b) Solution in G for the "expanding" problem.

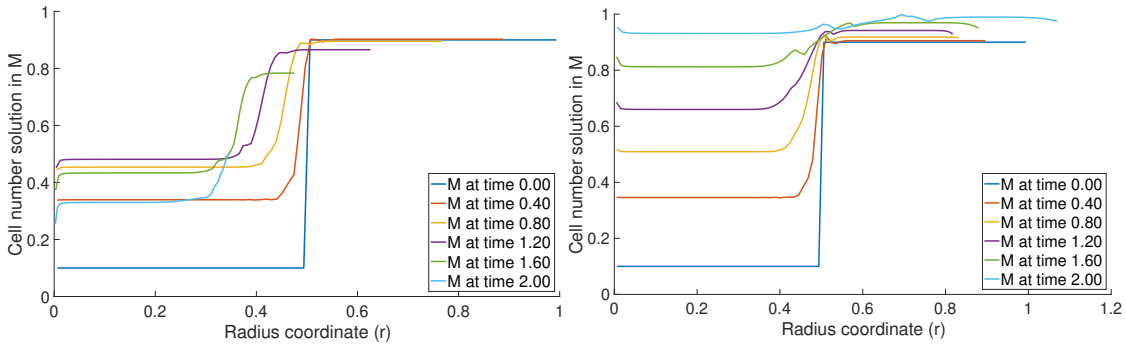

(c) Solution in M for the "shrinking" problem.

(d) Solution in M for the "expanding" problem.

Figure 2.2: The cell number solutions of the two tumor problems at different times computed on the finest grid with $N_\eta = 80$ uniform intervals.

the discontinuity, (b) the sum of the numerical data in G and M is very close to unity, and (c) in the "expanding" case, although the cell number G is pushed towards zero as time increases, the numerical solution stays positive. Note that (a) and (b) are expected from the construction of the segregate-flux method, see the analysis in [2]; in this thesis, we provide analysis of the positivity-preserving property of this method in Chapter 4 and thusly offer an explanation to the observation (c).

Chapter 3

Preliminary Mathematical Analysis

In this section we use the method of characteristics to conduct some preliminary analysis on the model problem (1.6) and attempt to justify the positivity of cell number solutions as well as the incompressibility condition, at least when solutions exist in the strong sense. Note that for practical problems, such an assumption is often unrealistic. Particularly when the immune cells actually infiltrate into the tumor (i.e., $u(1,\tau) < 0$), it tends to create a discontinuity in the cell number solutions. Biologically, such a discontinuity separate a low-density region of tumor cells nearby the origin and a high-density region nearby the tumor boundary, known as the "rim" [28]; and mathematically, it is a classical shock wave that propagates from the tumor boundary towards the origin.

Nevertheless, this chapter focuses on the rare situation when classical solution exists to gain better insight about the problem, whereas analysis of weak solutions as well as the entropy conditions are left for future work.

3.1 Characteristic analysis of the G-equation

First let us look at the G-equation (1.6a), which is rewritten as:

$$\frac{\partial G}{\partial \tau} + \left(\frac{V}{R} - \frac{\eta R'}{R}\right)\frac{\partial G}{\partial \eta} = \left[\hat{f}(G) - \frac{\eta V_\eta + 2V}{\eta R}\right] G\,. \tag{3.1}$$

To establish a local existence theory, let us fix η and consider the characteristics coordinate (ξ,τ), where ξ is defined by the path:

$$\frac{d\xi(\eta,\tau)}{d\tau} = -\xi\frac{R'(\tau)}{R(\tau)} + \frac{V(\xi,\tau)}{R(\tau)} \quad \text{with initial condition} \quad \xi(\eta,0) = \eta\,. \tag{3.2}$$

Then along the path defined by $\xi(\eta,\cdot)$, one has:

$$\frac{dG(\xi(\eta,\tau),\tau)}{d\tau} = \left[\hat{f}(G) - \frac{\xi V_\eta(\xi,\tau) + 2V(\xi,\tau)}{\xi R(\tau)}\right] G\,; \tag{3.3}$$

denoting the right-hand side by $a(\xi,\tau)G$, the solution to (3.3) is given by:

$$G(\xi(\eta,\tau),\tau) = G(\eta,0)e^{\int_0^\tau a(\xi(\eta,\tau'),\tau')d\tau'}\,, \tag{3.4}$$

hence $G(\xi,\tau) \geq 0$ for all $\tau \geq 0$ such that the characteristics do not break down.

The reason why the characteristic analysis may fail is the collision of the paths defined by (3.2). In particular, it is not difficult to see that $\xi(0,\tau) = 0$ and $\xi(1,\tau) = 1$ for all $\tau > 0$ such that $R(\tau) > 0$ and $V(\eta,\tau) < \infty$. Indeed, supposing $\eta = 0$ one easily sees that $\xi(0,\tau) = 0$ is a solution to (3.2) as $V(0,\tau) \equiv 0$. Similarly, assuming $\eta = 1$ one obtains immediately that $\xi(1,\tau) = 1$ solves (3.2) because $R'(\tau) = V(1,\tau)$. Then the uniqueness follows easily from the standard well-posedness theory of ordinary differential equations. Thus the previous analysis holds provided that $\eta \mapsto \xi$ gives an automorphism of $[0\,,1]$, which is valid if and only if:

$$\frac{\partial\xi(\eta,\tau)}{\partial\eta} > 0 \quad \text{ for all } \quad 0 \leq \eta \leq 1\,.$$

To this end, let us treat $\xi = \xi(\eta,\tau)$ as a bivariate function and taking the derivative w.r.t. η on both sides of (3.4) to obtain:

$$\frac{\partial\xi_\eta}{\partial\tau} = \xi_\eta\left(-\frac{R'(\tau)}{R(\tau)} + \frac{V_\eta(\xi,\tau)}{R(\tau)}\right)\,, \quad \xi_\eta(\eta,0) = 1\,.$$

Denoting the right hand side by $b(\xi,\tau)\xi_\eta$, one has:

$$\xi_\eta(\eta,\tau) = e^{\int_0^\tau b(\xi(\eta,\tau'),\tau')d\tau'}\,, \tag{3.5}$$

which is positive and finite as long as $b(\cdot,\cdot)$ remains bounded and integrable.

To summarize, we see that if $V \in C([0,T]\,,\, W^{1,\infty}([0,\ 1]))$, i.e., it is continuous in time and possesses bounded first spatial derivative, then $G(\eta,\tau) \geq 0,\ \forall(\eta,\tau) \in [0,1]\times[0,T]$ as long as $G(\eta,0) \geq 0,\ \forall\eta \in [0,1]$ and $R(\tau) > 0,\ \forall\eta \in [0,T]$.

3.2 Characteristic analysis of the M-equation

Now let us apply a similar analysis to the M-equation, which is rewritten as:

$$\frac{\partial M}{\partial \tau} + \left(\frac{V}{R} - \frac{\eta R'}{R} + \frac{u}{R}\right)\frac{\partial M}{\partial \eta} = \hat{h}_1(G,M)G + \left[\hat{h}_2(G,M) - \frac{\eta(V_\eta + u_\eta) + 2(V+u)}{\eta R}\right]M\,. \quad (3.6)$$

Because the advection velocity is different from that in (3.1), we need to define another set of characteristics ζ, such that:

$$\frac{\partial \zeta(\eta,\tau)}{\partial \tau} = -\zeta\frac{R'(\tau)}{R(\tau)} + \frac{V(\zeta,\tau)+u(\zeta,\tau)}{R(\tau)} \quad \text{with initial condition} \quad \zeta(\eta,0) = \eta\,. \quad (3.7)$$

Then along a path $\zeta(\eta,\cdot)$, one has:

$$\frac{dM(\zeta(\eta,\tau),\tau)}{d\tau} = \hat{h}_1 G + \left[\hat{h}_2 - \frac{\xi(V_\eta(\zeta,\tau)+u_\eta(\zeta,\tau)) + 2(V+u)(\zeta,\tau)}{\xi R(\tau)}\right]M\,. \quad (3.8)$$

Denoting the term in the square bracket by $c(\zeta,\tau)$, the solution to the ODE (3.8) is given:

$$M(\zeta(\eta,\tau),\tau) = M(\eta,0)e^{\int_0^\tau c(\zeta(\eta,\tau'),\tau')d\tau'} + \int_0^\tau e^{\int_{\tau'}^\tau c(\zeta(\eta,s),s)ds}\hat{h}_1 G(\zeta(\eta,\tau'),\tau')d\tau'\,. \quad (3.9)$$

By (1.2) we have $\hat{h}_1 \geq 0$, thus the positivity of G indicates that of M.

The characteristic analysis is valid only if the change of variable $\eta \to \zeta$ is well defined. Using the condition $u(0,\tau) = 0$ for all τ, we clearly see that $\zeta(0,\tau) = 0$. However, a major difference between the M-equation and the G-equation is that $\zeta(1,\tau) \not\equiv 1$. In fact, using $V(1,\tau) = R'(\tau)$ one obtains:

$$\frac{\partial \zeta(1,\tau)}{\partial \tau} = (1-\zeta)\frac{R'(\tau)}{R(\tau)} + \frac{u(\zeta,\tau)}{R(\tau)} \quad \text{with initial condition} \quad \zeta(1,0) = 1\,;$$

and $\zeta \equiv 1$ is the solution if and only if $u(1,\tau) = 0$.

For simplicity, let us assume $u(1,\tau)$ does not change signs (otherwise, we separate the time-axis into segments in each of which u does not change signs) and distinguish between two scenarios:

- $u(1,\tau) > 0$, $\forall\tau$. In this case, all information goes out of the tumor domain at $\eta = 1$ hence the validity of the characteristic analysis reduces to $\zeta_\eta(\eta,\tau) > 0$ for all $0 \leq \eta \leq 1$. Following a similar argument as before and taking derivative w.r.t. η in both sides of (3.7):

$$\frac{\partial \zeta_\eta}{\partial \tau} = \zeta_\eta\left(-\frac{R'(\tau)}{R(\tau)} + \frac{V_\eta(\zeta,\tau)+u_\eta(\zeta,\tau)}{R(\tau)}\right)\,, \quad 0 \leq \eta \leq 1\,,$$

we see that $\zeta_\eta > 0$ with sufficiently smooth V and u on the domain $\eta \in [0,\ 1]$.

- $u(1,\tau) < 0,\ \forall\tau$. In this case, all information comes into the domain at $\eta = 1$ hence there are possibly two characteristics emanating from this boundary. To the left of $\eta = 1$, which is denoted $\eta = 1^-$, V is well-defined hence one has for small τ:

$$\frac{\partial\zeta_\eta(1^-,\tau)}{\partial\tau} = \zeta_\eta(1^-,\tau)\left(-\frac{R'(\tau)}{R(\tau)} + \frac{V_\eta(\zeta(1^-,\tau),\tau) + u_\eta(\zeta(1^-,\tau),\tau)}{R(\tau)}\right),$$

whereas to the right of $\eta = 1$, which we denote by $\eta = 1^+$, V does not exists hence for small τ:

$$\frac{\partial\zeta_\eta(1^+,\tau)}{\partial\tau} = \zeta_\eta(1^+,\tau)\left(-\frac{R'(\tau)}{R(\tau)} + \frac{u_\eta(\zeta(1^+,\tau),\tau)}{R(\tau)}\right).$$

In order for ζ_η to be well-defined at $\eta = 1$, it is thusly necessary that:

$$V_\eta(1^-,\tau) + u_\eta(1^-,\tau) = u_\eta(1^+,\tau)\,, \tag{3.10}$$

which is unfortunately rarely true in practice. Indeed, in reality u is always obtained as the (negative) gradient of the chemoattractant, whose dynamics is governed by a standard diffusion process – hence u is usually very smooth at all η and $u_\eta < 0$. In this case, (3.10) is valid if and only if $V_\eta(1,\tau) = 0$. Let us consider the special case $f \equiv h \equiv 0$, by (1.10) this is equivalent to $u_\eta M + uM_\eta = 0$ at $\eta = 1$. However, it is frequently observed that M is nearly constant nearby $\eta = 1$ if $u(1,\tau) < 0$ and $m_{\mathrm{bc}}(\tau)$ is a constant; hence the previous condition holds if and only if $u_\eta = 0$, contradicting the observation $u_\eta < 0$.

3.3 The incompressibility assumption

In this section we prove the incompressibility constraint $\Theta \equiv 1$ when the solutions exist in the classical sense. The proof is based on the TCL (1.7) and the energy method. For preparation, the TCL is rewritten as:

$$\frac{\partial}{\partial\tau}[\eta^2 R^3(\Theta - 1)] + \frac{\partial}{\partial\eta}\left[(\eta^2 R^2 V - \eta^3 R' R^2)(\Theta - 1)\right] = 0\,, \tag{3.11}$$

Let us suppose that the solutions exist strongly and multiply (1.7) by $2(\Theta-1)$ and integrate the resulting equation over $\eta \in [0,\, 1]$. Using:

$$\begin{aligned}(\Theta-1)\frac{\partial}{\partial\tau}[\eta^2R^3(\Theta-1)] &= \frac{1}{2}\frac{\partial}{\partial\tau}[\eta^2R^3(\Theta-1)^2]+\frac{3}{2}\eta^2R'R^2(\Theta-1)^2\,,\\ (\Theta-1)\frac{\partial}{\partial\eta}[(\eta^2R^2V-\eta^3R'R^2)(\Theta-1)] &= \frac{1}{2}\frac{\partial}{\partial\eta}[(\eta^2R^2V-\eta^3R'R^2)(\Theta-1)^2]+\\ &\quad \frac{1}{2}(2\eta R^2V+\eta^2R^2V_\eta-3\eta^2R'R^2)(\Theta-1)^2\,,\end{aligned}$$

and defining the energy functional:

$$\mathscr{E}(\tau) \stackrel{\text{def}}{=\!=} \int_0^1 \eta^2R(\tau)^3(\Theta(\eta,\tau)-1)^2d\eta\,, \tag{3.12}$$

one obtains:

$$\mathscr{E}'(\tau) = -\int_0^1\left(\frac{2V}{\eta R}+\frac{V_\eta}{R}\right)\eta^2R^3(\Theta-1)^2d\eta\,,$$

where we used the fact that $\eta^2R^2V-\eta^3R'R^2=0$ at both $\eta=0$ and $\eta=1$. It follows that:

$$\mathscr{E}'(\tau) \le \frac{3\,||V_\eta||_\infty}{R(\tau)}\mathscr{E}(\tau)\,,$$

where $||\cdot||_\infty$ is the L_∞-norm and we used the mean value theorem and $V(0)=0$. By $\mathscr{E}(0)=0$ and the Grönwall's inequality, we have $\mathscr{E}(\tau)=0$ or equivalently $\Theta\equiv 1$ as long as $R(\tau)>0$.

Chapter 4

Numerical Positivity Preserving

In this section, we investigate under what conditions the numerical method will preserve the positivity of the cell number solutions, and how to enhance the scheme if the answer is no. For this purpose, it is assumed that the numerical solutions are positive at τ^n, i.e., $G^n_{j-\frac{1}{2}}, M^n_{j-\frac{1}{2}} > 0$ for all $1 \leq j \leq N_\eta$. The target is to ensure $G^{n+1}_{j-\frac{1}{2}} > 0$ and $M^{n+1}_{j-\frac{1}{2}} > 0$ for all j. To illustrate the idea of the analysis tool, we first focus on a some simpler case of linear advection equations and see that positivity preserving is equivalent to a classical Courant-like condition.

4.1 Advection equation with first-order upwind FVM

Let us consider the simple Cauchy problem for the advection equation on a fixed periodic domain that is discretized in space by the first-order upwind scheme:

$$\frac{\partial X}{\partial \tau} + v\frac{\partial X}{\partial \eta} = 0\,, \quad \eta \in [0,\,1]\,; \quad X(0,\tau) = X(1,\tau) \quad \forall \tau\,, \tag{4.1}$$

where v is a constant advection speed. Using the notations before, the semi-discretized and the fully-discretized solutions are denoted $X_{j-\frac{1}{2}}$ and $X^n_{j-\frac{1}{2}}$, respectively; here j and n are the indices for the spatial cell and the time stage.

Using the first-order upwind FVM in space, the fluxes are computed as:

$$F^X_j = \alpha^- X_{j-\frac{1}{2}} + \alpha^+ X_{j+\frac{1}{2}}\,,$$

where the α-coefficients are given by:

$$\alpha^- = \max(v,0) \geq 0\,, \quad \alpha^+ = \min(v,0) \leq 0\,. \tag{4.2}$$

Hence the ODE system after semi-discretization in space is given by:

$$\frac{dX_{j-\frac{1}{2}}}{d\tau}+\frac{1}{\Delta\eta}\left[\alpha^{+}X_{j+\frac{1}{2}}+(-\alpha^{+}+\alpha^{-})X_{j-\frac{1}{2}}-\alpha^{-}X_{j-\frac{3}{2}}\right]=0\,,\quad\forall j\,, \tag{4.3}$$

Now suppose the FE time-integrator is chosen, positivity preserving can be ensured if any discrete solution at τ^{n+1} is a convex combination of that at τ^{n}; and it often leads to a Courant-like condition. In particular, one has:

$$\frac{1}{\Delta\tau^{n}}\left(X^{n+1}_{j-\frac{1}{2}}-X^{n}_{j-\frac{1}{2}}\right)+\frac{1}{\Delta\eta}\left[\alpha^{+}X^{n}_{j+\frac{1}{2}}+(-\alpha^{+}+\alpha^{-})X^{n}_{j-\frac{1}{2}}-\alpha^{-}X^{n}_{j-\frac{3}{2}}\right]=0\,,\quad\forall j\,; \tag{4.4}$$

or equivalently:

$$X^{n+1}_{j-\frac{1}{2}}=-\alpha^{+}\frac{\Delta\tau}{\Delta\eta}X^{n}_{j+\frac{1}{2}}+\left[1-(-\alpha^{+}+\alpha^{-})\frac{\Delta\tau}{\Delta\eta}\right]X^{n}_{j-\frac{1}{2}}+\alpha^{-}\frac{\Delta\tau}{\Delta\eta}X^{n}_{j-\frac{3}{2}}\,. \tag{4.5}$$

Noticing $\alpha^{+}\leq 0$ and $\alpha^{-}\geq 0$, $X^{n+1}_{j-\frac{1}{2}}$ is a convex combination of $X^{n}_{j+\frac{1}{2}}$, $X^{n}_{j-\frac{1}{2}}$, and $X^{n}_{j-\frac{3}{2}}$ providing the classical Courant condition is satisfied:

$$|v|\,\Delta\tau\leq\Delta\eta\,, \tag{4.6}$$

where we used the fact that $-\alpha^{+}+\alpha^{-}=|v|$.

4.2 The first-order fluxes for the model problem

Extending the positivity-preserving analysis to the model problem follows a similar strategy - we attempt to write the solution at τ^{n+1} as a linear combination of those at τ^{n} with non-negative coefficients. We focus on the first-order upwind fluxes in this section; the third-order PPM flux will be discussed afterwards.

More specifically, the update equation for $G_{j-\frac{1}{2}}$ is written as:

$$\begin{aligned}\left(\frac{R^{n+1}}{R^{n}}\right)^{2}G^{n+1}_{j-\frac{1}{2}}=G^{n}_{j-\frac{1}{2}}&-\frac{\Delta\tau^{n}}{\Delta\eta\,\eta^{2}_{j-\frac{1}{2}}(R^{n})^{2}}\left[F^{G,n}_{V,j}+F^{G,n}_{R',j}-F^{G,n}_{V,j-1}-F^{G,n}_{R',j-1}\right]\\&+\Delta\tau^{n}\hat{f}^{n}_{j-\frac{1}{2}}G^{n}_{j-\frac{1}{2}}-\Delta\tau^{n}\frac{R'^{n}}{R^{n}}G^{n}_{j-\frac{1}{2}}\,,\end{aligned}$$

where $\hat{f}^n_{j-\frac{1}{2}} = \hat{f}(G^n_{j-\frac{1}{2}})$. The target is to write for each j:

$$F^{G,n}_{V,j} = \alpha^{n,-}_{V,j} G^n_{j-\frac{1}{2}} + \alpha^{n,+}_{V,j} G^n_{j+\frac{1}{2}} \,, \tag{4.7}$$

$$F^{G,n}_{R',j} = \alpha^{G,n,-}_{R',j} G^n_{j-\frac{1}{2}} + \alpha^{G,n,+}_{R',j} G^n_{j+\frac{1}{2}} \,. \tag{4.8}$$

Here the α-coefficients for the V-fluxes do not carry the letter G on their shoulder, as we will see later that these coefficients are identical across different cell species. However, if one casts the R'-flux that is computed by the PPM method (which has a much larger stencil) to the form (4.8), these coefficients are variable-dependent and thusly carry the superscript ^{G}. Denoting $\beta^n_{j-\frac{1}{2}} = \Delta\eta\,\eta^2_{j-\frac{1}{2}}(R^n)^2$ for simplicity, one can write $G^{n+1}_{j-\frac{1}{2}}$ as:

$$\begin{aligned}\left(\frac{R^{n+1}}{R^n}\right)^2 G^{n+1}_{j-\frac{1}{2}} = & \left[1 - \Delta\tau^n \left(\frac{\alpha^{n,-}_{V,j} + \alpha^{G,n,-}_{R',j} - \alpha^{n,+}_{V,j-1} - \alpha^{G,n,+}_{R',j-1}}{\beta^n_{j-\frac{1}{2}}} - \hat{f}^n_{j-\frac{1}{2}} + \frac{R'^n}{R^n}\right)\right] G^n_{j-\frac{1}{2}} \\ & + \frac{\Delta\tau^n}{\beta^n_{j-\frac{1}{2}}}\left[\left(\alpha^{n,-}_{V,j-1} + \alpha^{G,n,-}_{R',j-1}\right) G^n_{j-\frac{3}{2}} + \left(-\alpha^{n,+}_{V,j} - \alpha^{G,n,+}_{R',j}\right) G^n_{j+\frac{1}{2}}\right] .\end{aligned} \tag{4.9}$$

Hence a sufficient condition for the positivity of G is that all coefficients on the right-hand side are non-negative, among which the first term gives an upper bound for the size of $\Delta\tau^n$.

For the M-equation, we similarly obtain:

$$\begin{aligned}&\left(\frac{R^{n+1}}{R^n}\right)^2 M^{n+1}_{j-\frac{1}{2}} = \Delta\tau^n \hat{h}^n_{1,j-\frac{1}{2}} G^n_{j-\frac{1}{2}} \\ &+ \left[1 - \Delta\tau^n \left(\frac{\alpha^{n,-}_{V,j} + \alpha^{n,-}_{u,j} + \alpha^{M,n,-}_{R',j} - \alpha^{n,+}_{V,j-1} - \alpha^{n,+}_{u,j-1} - \alpha^{M,n,+}_{R',j-1}}{\beta^n_{j-\frac{1}{2}}} - \hat{h}^n_{2,j-\frac{1}{2}} + \frac{R'^n}{R^n}\right)\right] M^n_{j-\frac{1}{2}} \\ &+ \frac{\Delta\tau^n}{\beta^n_{j-\frac{1}{2}}}\left[\left(\alpha^{n,-}_{V,j-1} + \alpha^{n,-}_{u,j-1} + \alpha^{M,n,-}_{R',j-1}\right) M^n_{j-\frac{3}{2}} + \left(-\alpha^{n,+}_{V,j} - \alpha^{n,+}_{u,j} - \alpha^{M,n,+}_{R',j}\right) M^n_{j+\frac{1}{2}}\right] .\end{aligned} \tag{4.10}$$

where $\alpha^{n,\pm}_{u,k}$ are coefficients in constructing the fluxes $F^{M,n}_{u,k}$. As we assume $\hat{h}^n_{1,j-\frac{1}{2}} = \hat{h}_1(G^n_{j-\frac{1}{2}}) \geq 0$, positivity of the M-variables can again be derived from the non-negativity of the coefficients on the right-hand side.

In this section we focus on $\alpha^{n,\pm}_{V,j}$ and $\alpha^{n,\pm}_{u,j}$, both of which are constructed using the upwind flux hence they have similar structures. Letting X represent either G or M, the upwind flux $F^{X,n}_{V,j}$

is given by:

$$F_{V,j}^{X,n} = \eta_j^2 R^n \mathscr{F}^{\text{upw}}(X_{j-\frac{1}{2}}^n, X_{j+\frac{1}{2}}^n; V_j^n) = \begin{cases} \eta_j^2 R^n V_j^n X_{j-\frac{1}{2}}^n & \text{if} \quad V_j^n \geq 0\,, \\ \eta_j^2 R^n V_j^n X_{j+\frac{1}{2}}^n & \text{if} \quad V_j^n < 0\,. \end{cases} \tag{4.11}$$

Hence

$$\alpha_{V,j}^{n,-} = \eta_j^2 R^n \max(0, V_j^n) \geq 0\,, \quad \alpha_{V,j}^{n,+} = \eta_j^2 R^n \min(0, V_j^n) \leq 0\,. \tag{4.12}$$

Similarly for computing $F_{u,j}^{X,n}$, one has:

$$\alpha_{u,j}^{n,-} = \eta_j^2 R^n \max(0, u_j^n) \geq 0\,, \quad \alpha_{u,j}^{n,+} = \eta_j^2 R^n \min(0, u_j^n) \leq 0\,. \tag{4.13}$$

4.3 The PPM flux for the model problem

To write the flux associated with velocity R' as a linear combination of discrete solutions in a certain stencil, we briefly review how $F_{R',j}^{X,n}$ is computed by the PPM flux. Particularly, one has:

$$F_{R',j}^{X,n} = \mathscr{F}^{\text{upw}}(\overline{X}_{j-\frac{1}{2},+}^n, \overline{X}_{j+\frac{1}{2},-}^n; -R'^n R^n) = \alpha_R^{n,-} \overline{X}_{j-\frac{1}{2},+}^n + \alpha_R^{n,+} \overline{X}_{j+\frac{1}{2},-}^n\,, \tag{4.14}$$

where

$$\alpha_R^{n,-} = \max(0, -R'^n R^n) \geq 0\,, \quad \alpha_R^{n,+} = \min(0, -R'^n R^n) \leq 0\,. \tag{4.15}$$

Computing the "bar" variables involves average-preserving parabolic reconstruction of the solution on each interval, while using nonlinear limiters to ensure the reconstructed profile does not increase the total variation comparing to the piecewise constant discrete data before reconstruction. For our purpose, however, the key fact that $\left\{\overline{X}_{j-\frac{1}{2}}^n, \overline{X}_{j-\frac{1}{2},+}^n, \overline{X}_{j+\frac{1}{2},-}^n, \overline{X}_{j+\frac{1}{2}}^n\right\}$ always composes a monotone sequence, where for simplicity $\overline{X}$ denotes $\eta^3 X$, hence:

$$\overline{X}_{j-\frac{1}{2}}^n \overset{\text{def}}{=\!=} \eta_{j-\frac{1}{2}}^3 X_{j-\frac{1}{2}}^n\,, \quad \overline{X}_{j+\frac{1}{2}}^n \overset{\text{def}}{=\!=} \eta_{j+\frac{1}{2}}^3 X_{j+\frac{1}{2}}^n\,.$$

Hence there exist $0 \leq \gamma_{j,-}^{X,n} \leq \gamma_{j,+}^{X,n} \leq 1$, such that:

$$\overline{X}_{j-\frac{1}{2},+}^n = (1-\gamma_{j,-}^{X,n})\overline{X}_{j-\frac{1}{2}}^n + \gamma_{j,-}^{X,n}\overline{X}_{j+\frac{1}{2}}^n\,, \quad \overline{X}_{j+\frac{1}{2},-}^n = (1-\gamma_{j,+}^{X,n})\overline{X}_{j-\frac{1}{2}}^n + \gamma_{j,+}^{X,n}\overline{X}_{j+\frac{1}{2}}^n\,, \tag{4.16}$$

here γ is equipped with a superscript ^{X} as it depends on the variable and may not be the same across different cell species. Combining with (4.14) yields:

$$F^{X,n}_{R',j} = \left[\alpha^{n,-}_R(1-\gamma^{X,n}_{j,-}) + \alpha^{n,+}_R(1-\gamma^{X,n}_{j,+})\right]\eta^3_{j-\frac{1}{2}}X^n_{j-\frac{1}{2}} + \left[\alpha^{n,-}_R\gamma^{X,n}_{j,-} + \alpha^{n,+}_R\gamma^{X,n}_{j,+}\right]\eta^3_{j+\frac{1}{2}}X^n_{j+\frac{1}{2}}\,.$$

In comparison with (4.8), we get:

$$\begin{aligned}\alpha^{X,n,-}_{R',j} &= \left[\alpha^{n,-}_R(1-\gamma^{X,n}_{j,-}) + \alpha^{n,+}_R(1-\gamma^{X,n}_{j,+})\right]\eta^3_{j-\frac{1}{2}}\,,\\ \alpha^{X,n,+}_{R',j} &= \left[\alpha^{n,-}_R\gamma^{X,n}_{j,-} + \alpha^{n,+}_R\gamma^{X,n}_{j,+}\right]\eta^3_{j+\frac{1}{2}}\,.\end{aligned}$$

To this end, the conditions for the right-hand side of (4.9) consist of non-negative coefficients (except $G^n_{j-\frac{1}{2}}$, which is discussed later for the Courant condition) are listed below:

$$\begin{aligned}G^n_{j-\frac{3}{2}}:&\quad \alpha^{n,-}_{V,j-1} + \alpha^{G,n,-}_{R',j-1} \geq 0\,,\\ G^n_{j+\frac{1}{2}}:&\quad -\alpha^{n,+}_{V,j} - \alpha^{G,n,+}_{R',j} \geq 0\,.\end{aligned}$$

That is,

$$\begin{aligned}\eta^2_{j-1}R^n\max(0,V^n_{j-1}) + \left[\max(0,-R'^nR^n)(1-\gamma^{G,n}_{j-1,-}) + \min(0,-R'^nR^n)(1-\gamma^{G,n}_{j-1,+})\right]\eta^3_{j-\frac{3}{2}} \geq 0\,,\\ -\eta^2_jR^n\min(0,V^n_j) - \left[\max(0,-R'^nR^n)\gamma^{G,n}_{j,-} + \min(0,-R'^nR^n)\gamma^{G,n}_{j,+}\right]\eta^3_{j+\frac{1}{2}} \geq 0\,.\end{aligned}$$

A similar argument can be applied to the M-equation, so that we obtain the following requirements: If $R'^n < 0$, the first inequality holds naturally and the second one is equivalent to:

$$\gamma^{G,n}_{j,-} \leq \frac{-\eta^2_j\min(0,V^n_j)}{|R'^n|\eta^3_{j+\frac{1}{2}}}\,,\quad \gamma^{M,n}_{j,-} \leq \frac{-\eta^2_j(\min(0,V^n_j)+\min(0,u^n_j))}{|R'^n|\eta^3_{j+\frac{1}{2}}}\,, \tag{4.17}$$

whereas if $R'^n > 0$, the second inequality holds naturally and the first one is equivalent to:

$$1-\gamma^{G,n}_{j-1,+} \leq \frac{\eta^2_{j-1}\max(0,V^n_{j-1})}{|R'^n|\,\eta^3_{j-\frac{3}{2}}}\,,\quad 1-\gamma^{M,n}_{j-1,+} \leq \frac{\eta^2_{j-1}(\max(0,V^n_{j-1})+\max(0,u^n_{j-1}))}{|R'^n|\,\eta^3_{j-\frac{3}{2}}}\,. \tag{4.18}$$

Note that in the case of M, we also take into account of the infiltration velocity.

This suggests that while computing the PPM flux, one needs to take into account of the constraints (4.17) and (4.18), decreasing the limiter values if necessary. An enhancement to the flux computation is provided at the end of this section.

Once all the fluxes are computed such that (4.17) and (4.18) hold, the last piece in positivity-preserving is the non-negativity of the coefficient for $G^n_{j-\frac{1}{2}}$ and $M^n_{j-\frac{1}{2}}$ in the right-hand sides of (4.9) and (4.10), respectively. These lead to the following Courant condition for computing the time step size $\Delta\tau^n$:

$$\Delta\tau^n \le \left[\frac{(\alpha^{n,-}_{V,j} + \alpha^{n,-}_{R',j}) + (-\alpha^{n,+}_{V,j-1} - \alpha^{n,+}_{R',j-1})}{\beta^n_{j-\frac{1}{2}}} + L + \frac{\max(0, R'^n)}{R^n} \right]^{-1}, \tag{4.19}$$

$$\Delta\tau^n \le \left[\frac{(\alpha^{n,-}_{V,j} + \alpha^{n,-}_{u,j} + \alpha^{n,-}_{R',j}) + (-\alpha^{n,+}_{V,j-1} - \alpha^{n,+}_{u,j-1} - \alpha^{n,+}_{R',j-1})}{\beta^n_{j-\frac{1}{2}}} + L + \frac{\max(0, R'^n)}{R^n} \right]^{-1}. \tag{4.20}$$

Note that all terms in the parenthesis are non-negative by construction, and we've replaced the generic functions $\hat{f}$ and $\hat{h}_2$ by a universal estimate L, which may lead to a more conservative computation of the time step size but it is also easier to compute and implement.

4.4 An enhanced PPM flux with synchronized limiter

In this section, we'll describe an enhancement to the existing segregate-flux method such that the PPM fluxes are computed in a way such that (4.17) and (4.18) are satisfied.

To this end, we first review how the variables $\overline{X}^n_{j-\frac{1}{2},+}$ and $\overline{X}^n_{j+\frac{1}{2},-}$ in (4.14) are computed as well as the synchronized limiters.

(L1) Constructing third-order accurate values at η_j as:

$$\overline{X}^n_j = \frac{7}{12}(\overline{X}^n_{j-\frac{1}{2}} + \overline{X}^n_{j+\frac{1}{2}}) - \frac{1}{12}(\overline{X}^n_{j-\frac{3}{2}} + \overline{X}^n_{j+\frac{3}{2}}) .$$

(L2) To compute limiters $\phi^{X,n}_{j-\frac{1}{2},\pm} \in [0,\ 1]$ on each interval, we fist compute two parameters $\sigma^{X,n}_{j-\frac{1}{2},\pm} \ge 0$ as follows:

(L2-a) If $(\overline{X}^n_j - \overline{X}^n_{j-\frac{1}{2}})(\overline{X}^n_{j-1} - \overline{X}^n_{j-\frac{1}{2}}) \ge 0$:

$$\sigma^{X,n}_{j-\frac{1}{2},-} = \sigma^{X,n}_{j-\frac{1}{2},+} = 0 .$$

(L2-b) If (a) is not true, compute:

$$\sigma^{X,n}_{j-\frac{1}{2},+} = \frac{2\left|\overline{X}^n_{j-1} - \overline{X}^n_{j-\frac{1}{2}}\right|}{\left|\overline{X}^n_{j} - \overline{X}^n_{j-\frac{1}{2}}\right|}\,, \quad \sigma^{X,n}_{j-\frac{1}{2},-} = \frac{2\left|\overline{X}^n_{j} - \overline{X}^n_{j-\frac{1}{2}}\right|}{\left|\overline{X}^n_{j-1} - \overline{X}^n_{j-\frac{1}{2}}\right|}\,.$$

Then, the limiters are given by:

$$\phi^{X,n}_{j-\frac{1}{2},+} = \min\left(1, \sigma^{X,n}_{j-\frac{1}{2},+}\right)\,, \quad \phi^{X,n}_{j-\frac{1}{2},-} = \min\left(1, \sigma^{X,n}_{j-\frac{1}{2},-}\right)\,. \tag{4.21}$$

(L3) Compute the left- and right-extrapolated and limited values at each interval face:

$$\overline{X}^n_{j-\frac{1}{2},-} = \overline{X}^n_{j-\frac{1}{2}} + \phi^{X,n}_{j-\frac{1}{2},-}(\overline{X}^n_{j-1} - \overline{X}^n_{j-\frac{1}{2}})\,, \quad \overline{X}^n_{j-\frac{1}{2},+} = \overline{X}^n_{j-\frac{1}{2}} + \phi^{X,n}_{j-\frac{1}{2},+}(\overline{X}^n_{j} - \overline{X}^n_{j-\frac{1}{2}})\,.$$

Slight modifications are needed at both boundaries, more details can be found in [2].

A crucial ingredient in the segregate-flux method to achieve numerical incompressibility is to apply the same limiters to all cell species, a process called limiter synchronization. This can be achieved for the model problem as below:

(S1) Compute $\sigma^{G,n}_{j-\frac{1}{2},\pm}$ and $\sigma^{M,n}_{j-\frac{1}{2},\pm}$ as before.

(S2) Compute the "synchronized" parameters:

$$\sigma^{n}_{j-\frac{1}{2},+} = \min\left(\sigma^{G,n}_{j-\frac{1}{2},+}, \sigma^{M,n}_{j-\frac{1}{2},+}\right)\,, \quad \sigma^{n}_{j-\frac{1}{2},-} = \min\left(\sigma^{G,n}_{j-\frac{1}{2},-}, \sigma^{M,n}_{j-\frac{1}{2},-}\right)\,.$$

(S3) If $\sigma^{n}_{j-\frac{1}{2},+}\sigma^{n}_{j-\frac{1}{2},-} < 1$, set both of them to zero.

(S4) Compute the synchronized limiters:

$$\phi^{n}_{j-\frac{1}{2},+} = \min\left(1, \sigma^{n}_{j-\frac{1}{2},+}\right)\,, \quad \phi^{n}_{j-\frac{1}{2},-} = \min\left(1, \sigma^{n}_{j-\frac{1}{2},-}\right)\,. \tag{4.22}$$

Note that it is because of (S3) that we cannot compute the synchronized limiter by taking the minimum of the corresponding limiters across all cell species. In the original method $\phi^{n}_{j-\frac{1}{2},\pm}$ is applied to compute the R'-flux for both G and M, instead of using $\phi^{G,n}_{j-\frac{1}{2},\pm}$ and $\phi^{M,n}_{j-\frac{1}{2},\pm}$.

To enhance this method so that both (4.17) and (4.18) are satisfied, we first express $\gamma_{j,-}^{X,n}$ and $\gamma_{j,+}^{X,n}$ using the σ-parameters, where X represents either G or M:

$$\gamma_{j,-}^{X,n} = \frac{\overline{X}^n_{j-\frac{1}{2},+} - \overline{X}^n_{j-\frac{1}{2}}}{\overline{X}^n_{j+\frac{1}{2}} - \overline{X}^n_{j-\frac{1}{2}}} = \phi^n_{j-\frac{1}{2},+} \frac{\overline{X}^n_{j} - \overline{X}^n_{j-\frac{1}{2}}}{\overline{X}^n_{j+\frac{1}{2}} - \overline{X}^n_{j-\frac{1}{2}}},$$
$$\gamma_{j,+}^{X,n} = \frac{\overline{X}^n_{j+\frac{1}{2},-} - \overline{X}^n_{j-\frac{1}{2}}}{\overline{X}^n_{j+\frac{1}{2}} - \overline{X}^n_{j-\frac{1}{2}}} = 1 - \phi^n_{j+\frac{1}{2},-} \frac{\overline{X}^n_{j+\frac{1}{2}} - \overline{X}^n_{j}}{\overline{X}^n_{j+\frac{1}{2}} - \overline{X}^n_{j-\frac{1}{2}}}.$$

Hence the proposed modification follows the next steps:

(M1) Compute $\sigma^n_{j-\frac{1}{2},\pm}$ according to (S1)–(S3).

(M2) Update these two parameters as follows. If $R'^n < 0$:

$$\sigma^n_{j-\frac{1}{2},+} \leftarrow \min\left(\sigma^n_{j-\frac{1}{2},+}, \frac{-\eta_j^2 \min(0, V_j^n)}{|R'^n|\, \eta^3_{j+\frac{1}{2}}} \cdot \frac{\overline{G}^n_{j+\frac{1}{2}} - \overline{G}^n_{j-\frac{1}{2}}}{\overline{G}^n_{j} - \overline{G}^n_{j-\frac{1}{2}}}, \right.$$
$$\left. \frac{-\eta_j^2 (\min(0, V_j^n) + \min(0, u_j^n))}{|R'^n|\, \eta^3_{j+\frac{1}{2}}} \cdot \frac{\overline{M}^n_{j+\frac{1}{2}} - \overline{M}^n_{j-\frac{1}{2}}}{\overline{M}^n_{j} - \overline{M}^n_{j-\frac{1}{2}}} \right).$$

Otherwise (i.e., $R'^n > 0$):

$$\sigma^n_{j-\frac{1}{2},-} \leftarrow \min\left(\sigma^n_{j-\frac{1}{2},-}, \frac{\eta_{j-1}^2 \max(0, V_{j-1}^n)}{|R'^n|\, \eta^3_{j-\frac{3}{2}}} \cdot \frac{\overline{G}^n_{j-\frac{1}{2}} - \overline{G}^n_{j-\frac{3}{2}}}{\overline{G}^n_{j-\frac{1}{2}} - \overline{G}^n_{j-1}}, \right.$$
$$\left. \frac{\eta_{j-1}^2 (\max(0, V_{j-1}^n) + \max(0, u_{j-1}^n))}{|R'^n|\, \eta^3_{j-\frac{3}{2}}} \cdot \frac{\overline{M}^n_{j-\frac{1}{2}} - \overline{M}^n_{j-\frac{3}{2}}}{\overline{M}^n_{j-\frac{1}{2}} - \overline{M}^n_{j-1}} \right).$$

(M3) Repeat $(S3)$ and (S4).

We apply this modification to the numerical examples in Chapter 2.3, and obtain very similar results. This indicates that although a proof of positivity-preserving for the original segregate-flux method is lacking, its numerical performance largely resembles that of a positivity-preserving one, which partially explains why such a performance is observed in the previous numerical tests.

Chapter 5

Conclusions

In this thesis, we investigate two important properties of a tumor growth model that is due to immunce cell infiltration from both a mathematical point of view and by numerical methods. More specifically, the two properties are the positivity of cell number densities and the incompressibility that is assumed instead of enforced in the mathematical model.

From a mathematical perspective, we show that if the solutions in the strong form exist, they must satisfy both positivity for cell numbers and the cell incompressibility. In particular, the former is proved by a characteristic analysis for hyperbolic equations, whereas the latter is shown by an energy method. On the one hand, these results partially justify that the tumor model makes biological senses; on the other hand, due to the observation that solutions to these equations frequently exhibit discontinuities, the future work in this direction includes extending the analysis to weak solutions.

From a numerical point of view, a segregate-flux method was previously proposed by the advisor of the author such that cell incompressibility was maintained discretely. Furthermore, it was also observed that such numerical solutions always remain positive, even when they're pushed to extreme values such as that very close to zero. In this thesis, a proof to a slightly modified segregate-flux method is provided, to show that under a regular Courant condition for calculating the time step size, the cell number solutions at a new time step will remain positive as long as those at the previous time step are positive at all grid intervals.

References

[1] Ben Niu, Xianyi Zeng, Frank Szulzewsky, Sarah Holte, Philip K. Maini, Eric C. Holland, and Jianjun Paul Tian. Mathematical modeling of PDGF-driven glioma reveals the infiltrating dynamics of immune cells into tumors. 2018. Submitted.

[2] Xianyi Zeng, Mashriq Ahmed Saleh, and Jianjun Paul Tian. On finite volume discretization of infiltration dynamics in tumor growth models. Adv. Comput. Math., 45(5–6):3057–3094, 2019.

[3] Weber, G. F. The metastasis gene osteopontin:A candidate target for cancer therapy. 2001. Biochimica et Biophysica Acta - Reviews on Cancer. http://doi.org/10.1016/S0304-419X(01)00037-3

[4] Rittling, S. R., and Chambers, A. F. Role of osteopontin in tumour progression 2004. British Journal of Cancer http://doi.org/10.1038/sj.bjc.6601839

[5] Rangaswami, H., Bulbule A., and Kundu, G. C. Osteopontin: Role in cell signaling and cancer progression. 2006. Trends in Cell Biology http://doi.org/10.1016/j.tcb.2005.12.005

[6] Boon, T., Coulie, P. G., and Van Den Eynde, B. Tumor antigens recognized by T cells. 1997. Immunology Today http://doi.org/10.1016/S0167-5699(97)80020-5

[7] Gannot, G., Gannot, I., Vered, H., Buchner, A., and Keisari, Y. Increase in immune cell infiltration with progression of oral epithelium from hyperkeratosis to dysplasia and carcinoma. 2002. British Journal of Cancer http://doi.org/10.1038/sj.bjc.6600282

[8] Nosho, K., Baba, Y., Tanaka, N., Shima, K., Hayashi, M., Meyerhardt, J. A.,. . . Ogino, S. Tumour-infiltrating T-cell subsets, molecular changes in colorectal cancer, and prognosis: cohort study and literature review. 2010. J Pathol http://doi.org/10.1002/path.2774 [doi]

[9] Hald, J., Rasmussen, N., and Claesson, M. H. Tumour-infiltrating lymphocytesmediate lysis of autologous squamous cell carcinomas of the head and neck. 1995. Cancer Immunology Immunotherapy http://doi.org/10.1007/BF01516999

[10] Bram van Leer. Towards the ultimate conservative difference scheme V. A second-order sequel to Godunov's method. J. Comput. Phys., 32(1):101–136, July 1979.

[11] Jochems, C., and Schlom, J. Tumor-infiltrating immune cells and prognosis: The potential link between conventional cancer therapy and immunity. 2011. Experimental Biology and Medicine http://doi.org/10.1258/ebm.2011.011007

[12] McConkey J, Saleh S, Thompson D E. et al. Osteopontin regulates proliferation, apoptosis, and migration of murine claudin-low mammary tumor cells[J]. 2016. BMC cancer 16(1): 359

[13] Mantovani A., B. F. Inflammation and cancer 2001. The Lancet http://doi.org/10.1016/S0140-6736(00)04046-0

[14] Keller, E. F., and Segel, L. A. Model for chemotaxis. 1971. Journal of Theoretical Biology http://doi.org/10.1016/0022-5193(71)90050-6

[15] Quail, D., and Joyce, J. Microenvironmental regulation of tumor progression and metastasis. 2013. Nature Medicine http://doi.org/10.1038/nm.3394

[16] Whiteside TL. The tumor microenvironment and its role in promoting tumor growth. 2008.27(45):5904-12. Oncogene http://doi.10.1038/onc.2008.271

[17] Louis DN, Perry A, Reifenberger G, et al. The 2016 World Health Organization classification of tumors of the central nervous system: A summary. 2016;131(6):803-820 Acta Neuropathol

[18] McStay P, Green D. Measuring Apoptosis: Caspase Inhibitors and Activity Assays. 2014. Cold Spring Harbor Protoc. http://doi.10.1101/pdb.top070359

[19] Dorsey JF, Salinas RD, Dang M, et al. Cancer of the central nervous system. 2020. Elsevier In: Niederhuber JE, Armitage JO, Doroshow JH, Kastan MB, Tepper JE, eds. Abeloffs Clinical Oncology. 6th ed. Philadelphia, PA

[20] Phillip Colella and Paul R. Woodward. The piecewise parabolic method (ppm) for gas-dynamical simulations. J. Comput. Phys., 54(1):174–201, April 1984.

[21] Ben Niu, Xianyi Zeng, Tuan Anh Phan, Frank Szulzewsky, Sarah Holte, Eric C. Holland, and Jianjun Paul Tian. Mathematical modeling of PDGF-driven glioma reveals the dynamics of immune cells infiltrating into tumors. Neoplasia, 22(9):323–332, September 2020.

[22] Avner Friedman, Bei Hu, and Chuan Xue. Analysis of a mathematical model of ischemic cutaneous wounds. SIAM J. Math. Anal., 42(5):2013–2040, 2010. https://doi.org/10.1137/090772630.

[23] Avner Friedman, Wenrui Hao, and Bei Hu. A free boundary problem for steady small plaques in the artery and their stability. J. Differ. Equations, 259(4):1227–1255, August 2015. https://doi.org/10.1016/j.jde.2015.02.002.

[24] Avner Friedman. Mathematical Biology: Modeling and Analysis, volume 127 of CBMS Regional Conference Series in Mathematics. American Mathematical Society, June 2018.

[25] Randall LeVeque. Finite Volume Methods for Hyperbolic Problems. Cambridge Texts in Applied Mathematics. Cambridge University Press, 2002.

[26] S. K. Godunov. A difference scheme for numerical computation of discontinuous solution of hyperbolic equation. Matematicheskii Sbornik, 47(3):271–306, 1959.

[27] Phillip Colella and Michael D. Sekora. A limiter for PPM that preserves accuracy at smooth extrema. J. Comput. Phys., 227:7069–7076, 2008. Short Note.

[28] J. J. Casciari, S. V. Sotirchos, and R. M. Sutherland. Mathematical modelling of microenvironment and growth in EMT6/Ro multicellular tumour spheroids. Cell Proliferat., 25(1):1–22, January 1992.

Curriculum Vitae

Gilbert D. Acheampong was born on April 11, 1990. He completed his BSc. in Mathematics from the University for Development Studies, Ghana.

After working for 2 years with the Ghana Mathematics Society (Meagasa Math Academy) as a Teaching and Research Assistant, he proceeded to pursue a 1-Year Masters program in Mathematical Sciences at the African Institute for Mathematical Sciences, through the Next Einstein Initiative (NEI) Scholarship.

In Fall 2018, Gilbert gained admission and Graduate Assistantship offer to pursue the MS Math program at The University of Texas at El Paso. His research interests primarily falls within PDEs and Applied Analysis.

After graduation, he will be looking forward to starting a PhD program in Mathematics in Fall 2020.

Present address:
800 W Yandell Dr.
El Paso TX, 79902
gdacheampong@miners.utep.edu